Bioorganic & Medicinal Chemistry 18 (2010) 2076–2080

Contents lists available at ScienceDirect

Bioorganic & Medicinal Chemistry

journal homepage: www.elsevier.com/locate/bmc

Structural basis for the design of novel Schiff base metal chelate inhibitors of trypsin

Daisuke Iyaguchi, Susumu Kawano, Kazuki Takada, Eiko Toyota *

Faculty of Pharmaceutical Sciences, Health Sciences University of Hokkaido, Ishikari-Tobetsu, Hokkaido 061-0293, Japan

ARTICLE INFO

Article history:
Received 17 December 2009
Revised 8 February 2010
Accepted 9 February 2010
Available online 15 February 2010

Keywords:
Metal-mediated trypsin-inhibitors
Schiff base copper(II) chelates
X-ray crystallography
Structure–activity relationship

ABSTRACT

The crystal structures of the complexes of bovine trypsin with *m*-guanidinosalicylidene-L-alaninato(aqua)copper(II) hydrochloride (inhibitor 1), [*N*,*N*′-bis(*m*-guanidinosalicylidene)ethylenediaminato]copper(II) (inhibitor 2), and [*N*,*N*′-bis(*m*-amidinosalicylidene)ethylenediaminato]copper(II) (inhibitor 4) have been determined. The guanidine-containing trypsin-inhibitors (1 and 2) bind to the trypsin active site in a manner similar to that previously reported for amidine-containing inhibitors, for example, *m*-amidinosalicylidene-L-alaninato(aqua)copper(II) hydrochloride (inhibitor 3). However, the binding mode of the guanidino groups of inhibitors 1 and 2 to Asp189 in the S1 pocket of trypsin was found to be markedly different from that of the amidino group of inhibitor 3. The present X-ray analyses revealed that the interactions of the metal ion of the inhibitors with the active site residues of trypsin play a crucial role in the binding affinity to the trypsin molecule. These structural information and inhibitory activity data for amidine- and guanidine-containing Schiff base metal chelate inhibitors provide new avenues for designing novel inhibitors against physiologically important trypsin-like serine proteases.

1. Introduction

Trypsin is a member of a large and well-studied family of enzymes referred to as serine proteases. Studies on trypsin-specific compounds are useful for the design of clinically effective compounds since a variety of physiologically important enzymes (e.g., thrombin, kallikrein, and urokinase) have trypsin-like specificity.

It is well known that several benzamidine derivatives are potent competitive inhibitors of trypsin and trypsin-like enzymes. This strong inhibition arises from electrostatic interactions and bidentate hydrogen bonding between the carboxylate of Asp189, the hydroxyl oxygen of Ser190 and the carbonyl oxygen of Gly219, which are located at the bottom of the S1 site of trypsin, and the amidino group of the inhibitors.[1–5] We have reported the synthesis of amidine-containing Schiff base metal chelates and their inhibitory activity against trypsin and thrombin.[6–8] Many chelates prepared from various α-amino acids, metal ions, and benzamidine derivatives exhibited strong inhibitory activity against bovine trypsin and thrombin. To elucidate the structure–activity relationships of these inhibitors, we have studied the crystal structures of complexes between trypsin and amidine-containing Schiff base copper(II) or iron(III) chelates.[9] As a result, we have found a new mode of high affinity binding between trypsin and *m*-amidinosalicylidene-L-alaninato(aqua)copper(II) chelate (inhibitor 3). The copper(II) ion and phenolic oxygen of inhibitor 3 form additional interactions with the His57 and Ser195 residues of the active site besides the hydrogen-bonded salt bridge interactions between the amidino group and the Asp189 residue of the substrate binding site. This result suggests new avenues for the design of even more potent inhibitors based on combining a metal chelating motif with a cationic S1 recognition element. For example, guanidine-containing chelates may show higher affinity for trypsin than amidine-containing chelates as the chain length of the guanidino group [–NH–CH(NH_2)$_2$] is approximately 1.3 Å longer than that of the amidino group [–CH(NH_2)$_2$]. Furthermore, the guanidino group is more flexible than the amidino group. The increased length and the greater flexibility of the guanidino group compared with the amidino group may allow tighter coordination between the metal ion and the His57 and Ser195 residues within the active site of trypsin.

Previously, we reported the synthesis of guanidine-containing Schiff base metal chelates and their inhibitory activity towards trypsin.[10] Unexpectedly, the inhibitory activity of guanidine-containing metal chelates against trypsin was slightly less than that of the corresponding amidine-containing metal chelates. The present X-ray study was therefore undertaken in order to obtain direct evidence of guanidine-based inhibitor binding to trypsin and a strategy for the development of Schiff base metal chelate inhibitors. In this paper, we described the synthesis of new trypsin-inhibitors, 2 and 4, which carry two phenylguanidine moieties and two benzamidine moieties, respectively. The inhibition activi-

* Corresponding author. Tel.: +81 133 23 1211; fax: +81 133 23 1348.
E-mail address: toyota@hoku-iryo-u.ac.jp (E. Toyota).

0968-0896/$ - see front matter © 2010 Elsevier Ltd. All rights reserved.
doi:10.1016/j.bmc.2010.02.016

ties of four types of Schiff base metal chelate inhibitors (1–4) were determined and compared, and the crystal structures of trypsin bound to guanidine-containing inhibitors 1 and 2 were compared with the corresponding trypsin structures bound to amidine-containing inhibitors 3 and 4. The chemical structures and atom numbering of the inhibitors investigated in this study are shown in Figure 1.

2. Results

2.1. Synthesis of inhibitors (2, 4)

The structures of inhibitors 2 and 4 were assigned on the basis of their elemental analysis and spectral properties. The copper atom is coordinated to the two imino nitrogens and two phenolic oxygens of the *N*,*N*′-bis(*m*-guaninodisalicylidene)ethylenediaminato (inhibitor 2) or *N*,*N*′-bis(*m*-amidinosalicylidene)ethylenediaminato (inhibitor 4) ligand.[11–13]

2.2. Inhibitory activity towards trypsin

The inhibition constants (K_i value) of the inhibitors towards bovine trypsin were determined according to the reported procedure.[7,10] The K_i values of the guanidine-based inhibitors ($K_i = 3.1 \times 10^{-5}$ mol L^{-1} for inhibitor 1, 9.0×10^{-6} mol L^{-1} for inhibitor 2) were 10-fold smaller than those of the corresponding amidine-based inhibitors (2.8×10^{-6} mol L^{-1} for inhibitor 3, 2.4×10^{-7} mol L^{-1} for inhibitor 4). Thus, the inhibitory activity of the guanidine-based inhibitors (1 and 2) was weaker than that of the amidine-based inhibitors (3 and 4). Furthermore, the inhibitory activities of inhibitors 2 and 4 (ethylendiamine linked to two phenylguanidine rings or benzamidine rings) were stronger than those of inhibitors 1 and 3.

2.3. Binding of inhibitor 1 to trypsin

The crystal structure of trypsin bound to inhibitor 1 was solved by the molecular replacement method using the structure of PDB accession code 1G3D, which we previously reported to be the crystal structure of trypsin bound to inhibitor 3.[9] The electron density calculated with phases is well defined for trypsin and its inhibitor moieties, but that of the methyl group of its alanine moiety is poor. The hydrogen bonds and coordination bond distances in the active site of trypsin are summarized in Table 1. As expected, the copper(II) ion is close to the trypsin active site and directly coordinated to the imidazole nitrogen of His57, as is shown in Figure 2A, and its bond distance (2.3 Å) is shorter than that (3.1 Å) in the trypsin-inhibitor 3 complex (Fig. 2B, PDB accession code 1G3D).[9] The carbonyl oxygen of Ser214 also forms hydrogen bonds with the water molecule, which is coordinated to the copper ion. In addition, the chelate moiety is stabilized by the formation of hydrogen bonds between the phenolic oxygen (O1) of the inhibitor and the hydroxyl oxygen of Ser195 (2.3 Å). On the other hand, surprisingly, the guanidino group of the inhibitor does not form a bifurcated hydrogen-bonded salt bridge with the carboxylate of Asp189 at the bottom of the S1 pocket, which is a major interaction of inhibitor 3 with trypsin (Fig. 2B). Instead, the guanidino nitrogen atoms N1 and N2 form hydrogen bonds with the carboxylate oxygen of Asp189 (2.8 Å) and the carbonyl oxygen of Gly219 (2.4 Å), respectively. The N3 and N1 form additional water-mediated hydrogen bonds with the hydroxyl oxygen of Ser190.

2.4. Binding of inhibitor 2 to trypsin

The crystal structure of the trypsin active site region bound to inhibitor 2 is shown in Figure 3A. The electron density of the inhibitor moiety is well defined except for the ethylenediamine moiety and second guanidino group. Although the copper(II) ion is oriented toward the catalytic residues in the active site, no direct coordination bond between the copper(II) ion and the His57 or Ser195 catalytic residue was observed; whereas, the His57 and Ser195 residues do form hydrogen bonds with the phenolic oxygens (O1 and O2) of the inhibitor. As in the structure of the trypsin-inhibitor 1 complex, the three nitrogen atoms N1, N2, and N3 of the guanidino group form hydrogen bonds with the carboxylate

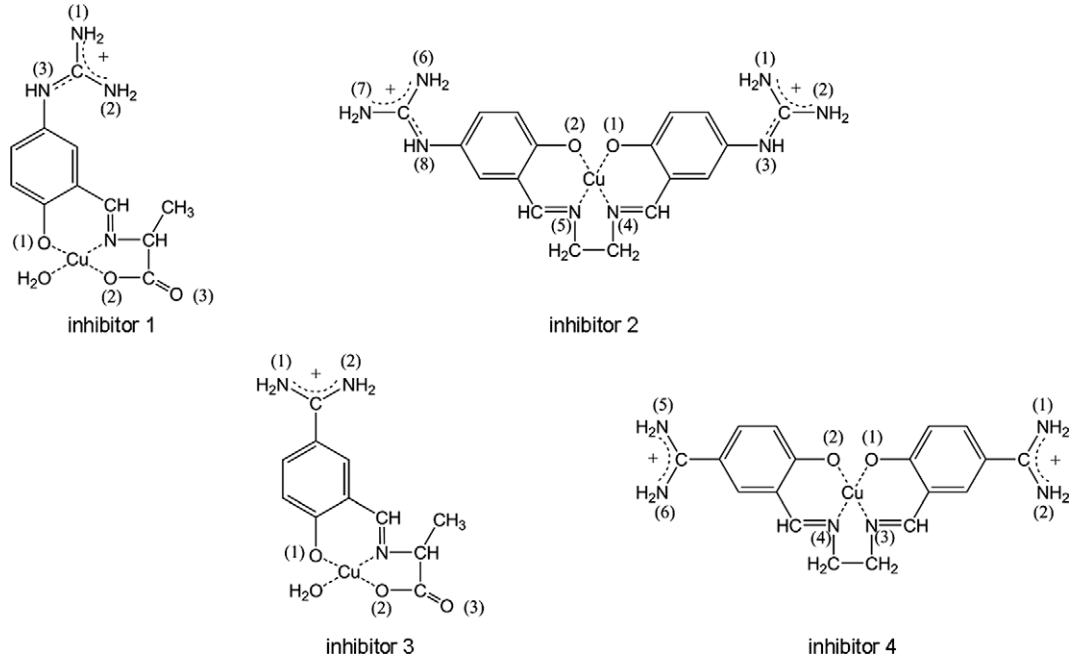

Figure 1. Chemical structures and atom numbering scheme for the inhibitors used in this study. Inhibitor 1: *m*-guanidinosalicylidene-L-alaninato(aqua)copper(II) hydrochloride, inhibitor 2: [*N*,*N*′-bis(*m*-guanidinosalicylidene)ethylenediaminato]copper(II), inhibitor 3: *m*-amidinosalicylidene-L-alaninato(aqua)copper(II) hydrochloride, inhibitor 4: [*N*,*N*′-bis(*m*-amidinosalicylidene)ethylenediaminato]copper(II).

Table 1
Hydrogen bonds and coordination bond distances

	Distance (Å)			
	Inhibitor 1	Inhibitor 2	Inhibitor 3[a]	Inhibitor 4
Ser195 O^{γ}-SB[b] O1	2.3	2.7	2.6	
Ser195 O^{γ}-Cu				2.6
His57N $^{\varepsilon 2}$-Cu	2.3		3.1	
His57N $^{\varepsilon 2}$-SB O2		3.1		3.0
Ser214 O-Water1	2.8	3.0	2.8	
Water1-Cu	2.8		2.4	
Asp189 $O^{\delta 2}$-SB N1	2.8	2.9	3.1	2.9
Asp189 $O^{\delta 1}$-SB N2			3.0	
Ser190 O-SB N1		3.0		
Ser190 O^{γ}-SB N1			2.8	3.1
Ser190 O^{γ}-SB N3		3.2		
Ser190 O^{γ}-Water2	2.2	2.8		
Val226 O-Water2		3.1		
Trp215 O-Water2		3.1		
Water2-SB N1	2.3			
Water2-SB N3	2.4	3.2		
Gly219 O-SB N1	3.2			
Gly219 O-SB N2	2.4	2.8	2.8	1.9

[a] PDB code 1G3D.
[b] SB, Schiff base.

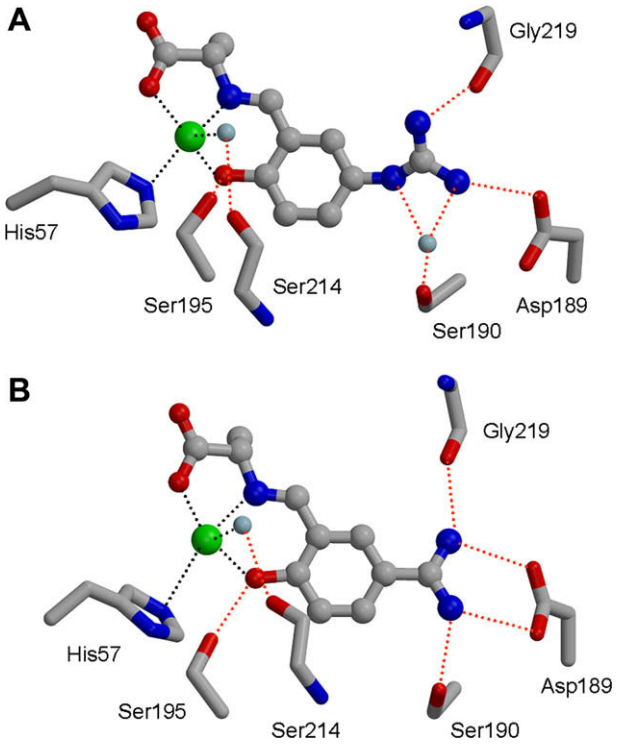

Figure 2. Detailed view of the interactions between guanidine-containing inhibitors and trypsin. (A) Trypsin-inhibitor 1 complex. (B) Trypsin-inhibitor 3 complex. Dashed red lines indicate hydrogen bonds. Coordination bonds are indicated as dashed black lines. Water molecules and the copper(II) ion are shown as light blue and green spheres, respectively. Residue numbers are labeled.

oxygen of Asp189, the carbonyl oxygen of Gly219, and the hydroxyl oxygen of Ser190, respectively. The N1 atom forms additional hydrogen bonds with the carbonyl oxygen of Ser190. The N3 atom also forms water-mediated hydrogen bonds with the carbonyl oxygens of Ser190, Trp215, and Val226. The second phenyl guanidine moiety of the inhibitor is directed into the cleft of the active site and has favorable van der Waals interactions with neighboring residues such as Phe41, Cys42, Cys58 and Lys60.

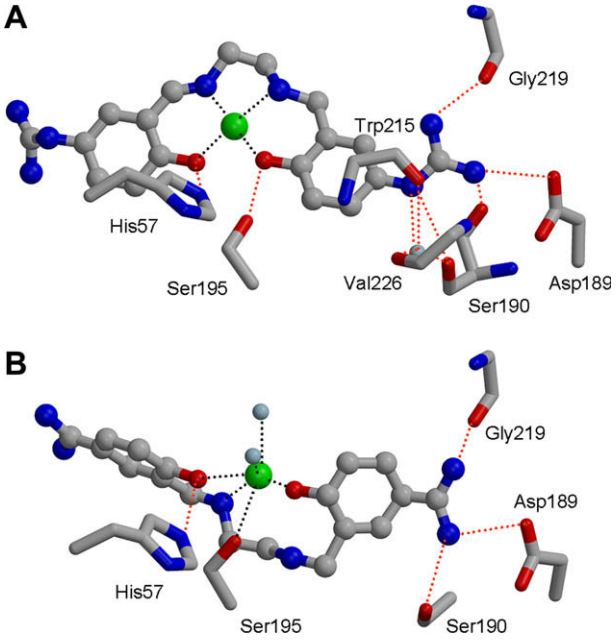

Figure 3. Detailed view of the interactions between amidine-containing inhibitors and trypsin. (A) Trypsin-inhibitor 2 complex. (B) Trypsin-inhibitor 4 complex. Dashed red lines indicate hydrogen bonds. Coordination bonds are indicated as dashed black lines. Water molecules and the copper(II) ion are shown as light blue and green spheres, respectively. Residue numbers are labeled.

2.5. Binding of inhibitor 4 to trypsin

The crystal structure of the trypsin active site region bound to inhibitor 4 is shown in Figure 3B. The electron densities of the inhibitor moieties are well defined except for those of the ethylenediamine and second benzamidine moieties. The amidino group of inhibitor 4 does not form a bifurcated hydrogen-bonded salt bridge with the carboxylate oxygen of Asp189. The nitrogen atoms of the amidino group bind to one of the carboxylate oxygens of Asp189, the hydroxyl oxygen of Ser190, and the carbonyl oxygen of Gly219. On the other hand, the coordination geometry of the copper(II) ion forms a distorted octahedral structure. The copper(II) ion binds to one of the imine nitrogens of ethylenediamine, the two phenolic oxygens of the salicylidene moiety, two water molecules, and the hydroxyl oxygen of Ser195. The distorted coordination geometry of copper(II) ion is caused by its interaction with Ser195. The imidazole nitrogen of His57 forms hydrogen bonds with phenolic oxygen. The second benzamidine moiety of the inhibitor is directed into the cleft of the active site and has favorable van der Waals interactions with neighboring active site residues.

3. Discussion

It is well known that the specific inhibition of amidine- or guanidine-based inhibitors toward trypsin or typsin-like enzymes is caused by forming a bifurcated hydrogen-bonded salt bridge between the cationic amidino or guanidino groups of the inhibitors and substrate binding site residues of enzymes, the anionic carboxylate of Asp189, the hydroxyl oxygen of Ser190, and the carbonyl oxygen of Gly219.[1–5,14–17] In our previous paper, we described a novel mode of potent inhibition of trypsin involving interaction between the metal ion of the inhibitors and the His57 side-chain of the trypsin active site.[9] It was expected that guanidine-containing chelates would have stronger interaction between the metal ion and active site residues than that of amidine-containing inhibitors as the chain length of the guanidine group is longer than that of the

amidino group. As expected, the copper ion of inhibitor 1 is coordinated by His57N$^{\varepsilon 2}$ (Fig. 2A). The Cu-His57N$^{\varepsilon 2}$ bond distance of inhibitor 1 (2.3 Å) bound to trypsin is shorter than that of inhibitor 3 (3.1 Å); however, the guanidino group of inhibitor 1 does not form a bifurcated hydrogen-bonded salt bridge with the substrate binding site residues. The conformation of the guanidino group of inhibitor 1 undergoes a large change to allow His57 to coordinate with the copper ion; thus, formation of the salt bridge between the guanidino group and Asp189 may be constrained. As a result, the binding affinity of inhibitor 1 ($K_i = 3.1 \times 10^{-5}$ mol L^{-1}) for trypsin is slightly lower than that of inhibitor 3 ($K_i = 2.8 \times 10^{-6}$ mol L^{-1}).

Compounds **2** and **4** were designed and synthesized as new potent trypsin-inhibitors. Inhibitors 2 and 4 have greater electrostatic interaction ability with trypsin than inhibitors 1 and 3, since these inhibitors (2 and 4) possess two cationic amidino or guanidino groups. Thus, it was expected that the binding affinities of inhibitors 2 and 4 for trypsin would be higher than those of the corresponding inhibitors 1 and 3. Inhibitory activity data showed that, as expected, the inhibition constants (K_i values) of inhibitor 2 (9.0×10^{-6} mol L^{-1}) and inhibitor 4 (2.4×10^{-7} mol L^{-1}) were smaller than those of inhibitors 1 (3.1×10^{-5} mol L^{-1}) and 3 (2.8×10^{-6} mol L^{-1}), respectively. In the crystal structure of inhibitor 2 bound to trypsin (Fig. 3A), the copper ion does not form any coordination bonds with the active site residues. The side-chains of His57 and Ser195 form hydrogen bonds with the two phenolic oxygens of the inhibitor. These interactions with active site residues are different from those in inhibitor 1. On the other hand, N1 and N2 nitrogen atoms of the guanidino group of inhibitor 2 form hydrogen bonds with a carboxylate oxygen of Asp189, the carbonyl oxygen of Gly219, and the carbonyl oxygen of Ser190, the same as trypsin-inhibitor 1 complex. The N3 nitrogen atom of the guanidino group forms additional hydrogen-bonded interactions with the hydroxyl oxygen of Ser190 and water-mediated hydrogen-bonded interactions with the carbonyl oxygens of Trp215 and Val226, compared with inhibitor 1 (Fig. 2A). Although the second guanidino group moiety does not form any hydrogen-bonded interaction with active site residues, the aromatic ring and ethylenediamine moieties of inhibitor 2 have favorable van der Waals interactions with some neighboring active site residues, such as Phe41, Cys42, Cys58 and Lys60. Thus, these additional interactions of inhibitor 2 result in slightly higher binding affinity than that of inhibitor 1. In the crystal structure of inhibitor 4 bound to trypsin (Fig. 3B), the amidino group of the inhibitor does not form a bifurcated hydrogen-bonded salt bridge with Asp189. Amidino nitrogen atoms form hydrogen bonds with one of the carboxylate oxygens of Asp189, the hydroxyl oxygen of Ser190, and the carbonyl oxygen of Gly219. On the other hand, the copper ion of the inhibitor is directly coordinated to the hydroxyl oxygen of Ser195 (2.6 Å). Furthermore, the second benzamidine and ethylenediamine moieties of the inhibitor have favorable van der Waals interactions with neighboring active site residues. Thus, these additional van der Waals interactions and the coordination bond of Cu-Ser195O$^{\gamma}$ must produce a higher binding affinity of inhibitor 4 ($K_i = 2.4 \times 10^{-7}$ mol L^{-1}) than that of inhibitor 3 ($K_i = 2.8 \times 10^{-6}$ mol L^{-1}).

From the results of this study, it is clear that the interactions between the metal ion and the active site residues (e.g., His57, Ser195) play a crucial role in the binding affinity of inhibitors to the trypsin molecule, as well as the bifurcated hydrogen-bonded salt bridge interactions between the amidino or guanidino group of the inhibitor and the substrate binding site residues of trypsin. The bifurcated interaction (as seen in inhibitor 3) is known to be the most important interaction in this type of inhibitor.[1–5] In the inhibitor 1-trypsin complex, although bifurcated interaction is disrupted, a high level of inhibitory activity towards trypsin is maintained. This indicates that increased interaction between the metal ion and the active site residue (Cu-His57) compensates for loss of the interaction in the substrate binding site. Inhibitor 4 has strong inhibitory activity towards trypsin. In the inhibitor 4-trypsin complex, the copper(II) ion binds directly to the hydroxyl oxygen of Ser195. This result supports the idea that the interaction between the metal ion and active site residues is a key component in their inhibitory activity.

Our current study suggests new avenues for the design of even more potent inhibitors based on combining a metal chelating motif with a cationic S1 recognition element. The synthetic route adopted for our inhibitors offers great promise for the facile synthesis of a wide range of inhibitors by combining different amino acids, metal ions, and cationic organic moieties. This approach will hopefully lead to the development of more potent inhibitors targeting other physiologically important enzymes, as well as trypsin-like proteases.

4. Experimental

4.1. Instruments

Melting points were measured on a Yanagimoto micro melting point apparatus. IR and absorption spectra were recorded on an FT/IR-460 spectrometer (JASCO) and a V-630 BIO spectrophotometer (JASCO), respectively.

4.2. Synthesis of inhibitor

m-Guanidinosalicylidene-L-alaninato(aqua)copper(II) hydrochloride (inhibitor 1) and *m*-amidinosalicylidene-L-alaninato(aqua)copper(II) hydrochloride (inhibitor 3) were prepared according to the reported procedures.[7,10]

4.2.1. [*N*,*N*′-Bis(*m*-guanidinosalicylidene)ethylenediaminato]-copper(II) hydrate (inhibitor 2)

A solution of ethylenediamine (0.06 g, 1.0 mmol) in EtOH (3.0 mL) was added to 3-formyl-4-hydroxyphenylguanidine hydrochloride (0.43 g, 2.0 mmol) in water (3 mL) and stirred for 10 min at 50 °C. To the reaction mixture, a solution of copper(II) acetate monohydrate (0.2 g, 1.0 mmol) in water (2 mL) was added over 15 min. The solution was stirred for 2 h at 50 °C and evaporated to dryness. The complex was purified by recrystallization from H_2O–acetone and dried under a vacuum. A grayish violet crystalline powder was obtained (0.36 g, 80.7%). mp (dec.): 200–203 °C; IR (KBr) 3200–3600 cm^{-1} ($\nu(H_2O)$ and ν(NH)), 1654 cm^{-1}, 1638 cm^{-1}; Absorption spectra (H_2O): 345 nm ($\varepsilon = 4510$), 564 nm ($\varepsilon = 218$). Anal. Calcd for $C_{18}H_{22}CuN_8O_3$: C, 46.79; H, 4.80; N, 24.26. Found: C, 46.44; H, 5.03; N, 23.98.

4.2.2. [*N*,*N*′-Bis(*m*-amidinosalicylidene)ethylenediaminato]-copper(II) (inhibitor 4)

The synthesis of inhibitor 4 was carried out in the same manner as for inhibitor 2 using 3-formyl-4-hydroxybenzamidine hydrochloride. The complex was purified by recrystallization from H_2O–EtOH and dried under a vacuum. A purple crystalline powder was obtained (0.26 g, 62.8%). mp (dec.): 215–217 °C; IR (KBr) 3300–3600 cm^{-1}, 1638 cm^{-1}, 1618 cm^{-1}; Absorption spectra (H_2O): 340 nm ($\varepsilon = 4500$), 545 nm ($\varepsilon = 210$). Anal. Calcd for $C_{18}H_{18}CuN_6O_2$: C, 52.23; H, 4.38; N, 20.30. Found: C, 51.92; H, 4.22; N, 20.19.

4.3. Determination of inhibition constant (K_i) of chelates for trypsin

The inhibition constants (dissociation constants) of inhibitors 1–4 for trypsin were determined from rate assays employing benzoyl-L-arginine *p*-nitroanilide (BAPA) as a substrate. All the che-

lates behaved as competitive inhibitors for trypsin with K_i values in the range of 10^{-5}–10^{-7} mol L^{-1}.

4.4. Crystallization of trypsin-inhibitor complex

Bovine β-trypsin was purchased from Sigma (Type XIII). The co-crystallization of trypsin-inhibiter complexes was performed by the hanging-drop vapor diffusion method at 20 °C. Crystals of trypsin-inhibitor 1 complex (trypsin-1) were obtained by equilibrating droplets containing 1.25 mM trypsin, 2.5 mM inhibitor 1, 6 mM $CaCl_2$, and 100 mM Tris–HCl buffer (pH 8.0) against a reservoir solution containing 100 mM Tris–HCl buffer (pH 8.0), 200 mM Li_2SO_4 and 26% PEG 4000. Crystals of trypsin-inhibitor 2 complex (trypsin-2) were obtained by equilibrating droplets containing 1.25 mM trypsin, 2.5 mM inhibitor 2, 6 mM $CaCl_2$, and 100 mM Tris–HCl buffer (pH 8.0) against a reservoir solution containing 100 mM Tris–HCl buffer (pH 8.0), 200 mM Li_2SO_4 and 22% PEG 4000. Crystals of trypsin-inhibitor 4 complex (trypsin-4) were obtained from 1.25 mM trypsin, 2.5 mM inhibitor 4, 6 mM $CaCl_2$, and 100 mM Tris–HCl buffer (pH 8.0) against a reservoir solution containing 100 mM Tris–HCl buffer (pH 8.0), 200 mM Li_2SO_4 and 22% PEG 4000.

4.5. Crystallographic data collection and structural refinements

Complete X-ray diffraction data for trypsin-1, trypsin-2, and trypsin-4 were collected using an R-AXIS IV^{++} image-plate detector at 1.75 Å, 1.80 Å, and 1.70 Å resolution, respectively. The diffraction experiments were performed under cryocooling conditions (100 K) after the crystals had been soaked in a cryoprotectant solution containing 20% glycerol mixed with the reservoir solution. The diffraction images were analyzed and processed using the HKL2000 program.[18] These crystals belonged to the space group $P2_12_12_1$ for trypsin-1 and trypsin-2, and $P3_1$ for trypsin-4. The unit cell parameters for the crystals are given in Table 2. These parameters indicate one molecule per asymmetric unit for trypsin-1 and trypsin-2 and two molecules for trypsin-4 with V_M values of 2.08 (Å^3/Da), 2.19 (Å^3/Da), and 2.22 (Å^3/Da), respectively, based on an estimated molecular mass of 24 kDa.[19] The data collection statistics are summarized in Table 2. The structures were solved by molecular replacement using the program AMORE[20] with the crystal structure of trypsin-inhibitor 3 complex (PDB code 1G3D)[9] as a search model. Structural refinement was performed using the program LAFIRE[21] and CNS[22] with manual interventions of the model modification using the program O.[23] Analysis of the protein geometry was performed using the program PROCHECK.[24] Refinement statistics are summarized in Table 2. The atomic coordinates of trypsin-inhibitor 1, trypsin-inhibitor 2, and trypsin-inhibitor 4 have been deposited in the Protein Data Bank under accession codes 3AAS, 3AAU, and 3AAV, respectively.

Table 2
Crystallographic data and refinement statistics

	Inhibitor 1	Inhibitor 2	Inhibitor 4
Data collection statistics[a]			
Space group	$P2_12_12_1$	$P2_12_12_1$	$P3_1$
Cell parameters			
a (Å)	54.0	54.2	54.6
b (Å)	56.3	58.4	54.6
c (Å)	65.7	66.5	107.2
Wavelength (Å)	1.54	1.54	1.54
Total reflections	131,509	206,858	437,553
Unique reflections	20,227	19,852	39,258
Resolution (Å)	50.0–1.75 (1.81–1.75)	50.0–1.80 (1.86–1.80)	50.0–1.70 (1.76–1.70)
Completeness (%)	97.0 (95.0)	98.3 (96.6)	99.9 (100.0)
Redundancy	6.5 (6.9)	10.4 (10.5)	11.1 (10.7)
R_{merge}[b] (%)	5.7 (19.1)	9.6 (30.3)	5.8 (21.3)
Refinement statistics			
Resolution (Å)	20.0–1.75	20.0–1.80	20.0–1.70
R factor[c]/R_{free}[d] (%)	17.3/20.9	17.3/20.2	18.4/21.0
No. of amino acid residues	223	223	223 × 2
No. of inhibitor molecules	1	1	2
No. of calcium ions	1	1	2
No. of solvent atoms	275	259	402
Rmsd from ideal			
Bond lengths (Å)	0.0047	0.0045	0.0049
Bond angles (°)	1.353	1.380	1.385
Average *B* factor (Å^2)	20.87	17.86	20.47
Ramachandran plot (%)			
Most favored	85.6	86.7	85.1
Add. allowed	14.4	13.3	14.1

Rmsd, root mean square deviation.

[a] Values in parentheses are for the highest resolution shell.

[b] $R_{merge} = \{\sum_h\sum_i |<I(h)> - I(h)_i|\}/\sum_h\sum_i I(h)_i$, where $I(h)_i$ is the *i*th observation of reflection *h* and $<I(h)>$ is the mean intensity of all observations of reflection *h*.

[c] *R* factor = $\{\sum||F_{obs}| - |F_{calc}||\}/\sum|F_{obs}|$, where $|F_{obs}|$ and $|F_{calc}|$ are observed and calculated structure factor amplitudes.

[d] R_{free} was calculated for 10% randomly selected reflections of data sets that were not used in the refinement.

Acknowledgments

This work was supported by the High Technology Research Program from the Ministry of Education, Culture, Sports, Science and Technology of Japan.

References and notes

1. Turk, D.; Stürzebecher, J.; Bode, W. *FEBS Lett.* **1991**, *287*, 133.
2. Renatus, M.; Bode, W.; Huber, R.; Stürzebecher, J.; Stubbs, M. *J. Med. Chem.* **1998**, *41*, 5445.
3. Katz, B. A.; Clark, J. M.; Finer-Moore, J. S.; Jenkins, T. E.; Johnson, C. R.; Ross, M. J.; Luong, C.; Moore, W. R.; Stroud, R. M. *Nature* **1998**, *391*, 608.
4. Katz, B. A.; Luong, C. *J. Mol. Biol.* **1999**, *292*, 669.
5. Nilsson, J. W.; Kvarnström, I.; Musil, D.; Nilsson, I.; Samulesson, B. *J. Med. Chem.* **2003**, *46*, 3985.
6. Toyota, E.; Chinen, C.; Sekizaki, H.; Itoh, K.; Tanizawa, K. *Chem. Pharm. Bull.* **1996**, *44*, 1104.
7. Toyota, E.; Miyazaki, H.; Itoh, K.; Sekizaki, H.; Tanizawa, K. *Chem. Pharm. Bull.* **1999**, *47*, 116.
8. Toyota, E.; Sekizaki, H.; Takahashi, Y.; Itoh, K.; Tanizawa, K. *Chem. Pharm. Bull.* **2005**, *53*, 22.
9. Toyota, E.; Ng, K. K.; Sekizaki, H.; Itoh, K.; Tanizawa, K.; James, M. N. *J. Mol. Biol.* **2001**, *305*, 471.
10. Toyota, E.; Sekizaki, H.; Itoh, K.; Tanizawa, K. *Chem. Pharm. Bull.* **2003**, *51*, 625.
11. Llewellyn, J.; Waters, T. N. *J. Chem. Soc.* **1960**, 2639.
12. Hall, D.; Waters, T. N. *J. Chem. Soc.* **1960**, 2644.
13. Drew, M. G. B.; Prasad, R. N.; Sharma, R. P. *Acta Crystallogr., Sect. C* **1985**, *41*, 1755.
14. Matsumoto, O.; Taga, T.; Matsushima, M.; Higashi, T.; Machida, K. *Chem. Pharm. Bull.* **1990**, *38*, 2253.
15. Mangel, W. F.; Singer, P. T.; Cyr, D. M.; Umland, T. C.; Toledo, D. L.; Stroud, R. M.; Pflugrath, J. W.; Sweet, R. M. *Biochemistry* **1990**, *29*, 8351.
16. Odagaki, Y.; Nakai, H.; Senokuchi, K.; Kawamura, M.; Hamanaka, N.; Nakamura, M.; Tomoo, K.; Ishida, T. *Biochemistry* **1995**, *34*, 12849.
17. Sperl, S.; Jacob, U.; Prada, N. A.; Stürzebecher, J.; Wiilhelm, O. G.; Bode, W.; Magdolen, V.; Huber, R.; Moroder, L. *Proc. Natl. Acad. Sci. U.S.A.* **2000**, *97*, 5113.
18. Otwinowski, Z.; Minor, W. *Methods Enzymol.* **1997**, *276*, 307.
19. Matthews, B. W. *J. Mol. Biol.* **1968**, *33*, 491.
20. Navaza, J. *Acta Crystallogr., Sect. A* **1994**, *50*, 157.
21. Yao, M.; Zhou, Y.; Tanaka, I. *Acta Crystallogr., Sect. D* **2006**, *62*, 189.
22. Brunger, A. T.; Adams, P. D.; Clore, G. M.; Delano, W. L.; Gros, P.; Grosse-Kunstleve, R. W.; Jiang, J. S.; Kuszewski, J.; Nilges, M.; Pannu, N. S.; Read, R. J.; Rice, L. M.; Simonson, T.; Warren, G. L. *Acta Crystallogr., Sect. D* **1998**, *54*, 905.
23. Jones, T. A.; Zou, J. Y.; Cowan, S. W.; Kjeldgaard, M. *Acta Crystallogr., Sect. A* **1991**, *47*, 110.
24. Laskowski, R. A.; MacArthur, M. W.; Moss, D. S.; Thornton, J. M. *J. Appl. Crystallogr.* **1993**, *26*, 283.